

# MAGNETIC FIELD MEASUREMENTS OF THE INITIAL FERMILAB MAIN INJECTOR PRODUCTION DIPOLES\*

D.J. Harding, R. Baiod, B.C. Brown, J.A. Carson, N.S. Chester, E. Desavouret, J. DiMarco, J.D. Garvey, H.D. Glass, P.J. Hall, P.S. Martin, P.O. Mazur, C.S. Mishra, A. Mokhtarani, J.M. Nogiec, D.F. Orris, J.E. Pachnik, A.D. Russell, S.A. Sharonov, J.W. Sim, J.C. Tompkins, K. Trombly-Freytag, D.G.C. Walbridge, and V.A. Yarba, Fermi National Accelerator Laboratory\*, P.O. Box 500, Batavia, IL 60510 USA

## Abstract

A large sample of the 6-meter dipoles for the Fermilab Main Injector have been fabricated and measured. The resulting properties are reported and compared to the accelerator requirements.

## I. Magnet requirements

The Fermilab Main Injector is a new proton and antiproton accelerator currently under construction at Fermi National Accelerator Laboratory [1]. It will replace the existing Main Ring in all functions. While many of the Main Ring quadrupoles will be reused in the Main Injector, the dipoles are a new design. The performance requirements of the dipoles have been studied extensively [2]. The two significant areas of magnetic performance are the magnet-to-magnet variation in the integrated magnetic field (“strength”) and the variation of the strength as a function of transverse position (“shape”). We discuss these topics separately here.

### A. Strength

We define the strength to be  $\int_{-\infty}^{\infty} B_y dz$ . The integral is taken at the center of the aperture and follows the path of the central orbit, curving with the magnet. We quote relative strengths in “units” of parts in  $10^4$ .

Based on experience, we expected to be able to limit the variation in strength to 10 units ( $10 \times 10^{-4}$ ). The majority of our tracking studies have used the more generous assumption of a root mean square deviation of 10 units and have found that with that distribution no selection of magnets for placement in the ring is necessary. We have also tried a broader Gaussian distribution with  $\sigma=15$  units and a bimodal distribution with two narrow peaks separated by 30 units [3]. In the former case, we can expect the planned trim dipoles to correct the closed orbit even with random assignment of the dipoles. In the latter case, a simple magnet placement plan is needed.

### B. Shape

We define the shape to be the variation in the strength as a function of transverse position. We characterize the shape by the horizontal variation  $\int_{-\infty}^{\infty} B_y(x) dz$  of the field integral and by the harmonic decomposition of the integral. We can link the two by writing

$$B_y(x) = B_0 \left( 1 + b_2 \left( \frac{x}{r_0} \right)^2 + b_4 \left( \frac{x}{r_0} \right)^4 + \dots \right),$$

where  $B_y(x)$  is the integral,  $B_0$  is the strength, and  $b_n$  are the normal harmonic components. We quote the components at  $r_0 = 25.4$  mm and in “units” of parts in  $10^4$ .

From the symmetry of the magnet design we expect the field to be both left-right and up-down symmetrical. For our tracking studies we have assumed distributions of the forbidden components that are consistent with the measured spread in values without questioning whether these values are real or primarily measurement error, either random or systematic. The measured values are small. We concentrate here on the allowed components.

The chromaticity sextupole system [4] is designed to compensate for the average size of the sextupole component of the dipoles. The accelerator is not very sensitive to variations in the sextupole around the ring. The decapole component is clearly measurable, but not large enough to pose a problem for the accelerator.

## II. Measurement systems

The equipment and software used in measuring the magnets is described with more detail in other papers at this conference and elsewhere [5]. The request from the Main Injector project was that every magnet be measured and that in production the strength and shape be determined by at least two independent methods. A third strength measurement is used on a sample of magnets for further redundancy.

The flatcoil system uses a long, narrow, multi-turn coil that extends through the length of the magnet, performing the integral over  $z$ . The coil form is rigid and curved to match the central orbit of a particle through the curved magnet. The magnet strength, exclusive of the remanent field, is determined by measuring the change in flux through the coil as the magnet is excited with the probe held in the center of the magnet. The horizontal variation in the field is determined by measuring the change in flux as the probe is moved laterally with the current held fixed. A polynomial fit to the shape data yields coefficients proportional to the normal coefficients of a harmonic decomposition of the magnetic field. The flatcoil measurements are performed at multiple currents on every magnet.

The rotating coil system uses a tangential coil that extends through the length of the magnet. The G-10 coil form has a small enough diameter that it easily conforms to the curved central orbit of the magnet and flexes as it is rotated to maintain the curvature. A coil wound on one diameter of the probe provides a measurement of the absolute strength of the magnet. The tangential coil, bucked against the equal-area diameter coil, pro-

\*Work supported by the United States Department of Energy under contract No. DE-AC02-76CH03000

vides flux measurements on a circle, from which the normal and skew harmonic components are extracted. The rotating coil measurements are performed at multiple currents on every magnet.

The pointscan system uses both a Hall probe and an NMR probe to scan the magnetic field along the magnet's length in 25.4 mm steps. Numerically integrating the field measurements gives the magnet strength. These time-consuming pointscan measurements are performed at two currents on a sample of magnets.

### III. Measurement Data

#### A. Strength

For each measurement system we have averaged the strength at each current. Figure 1 shows the deviation of the average strength from a linear excitation calculated assuming infinite steel permeability.

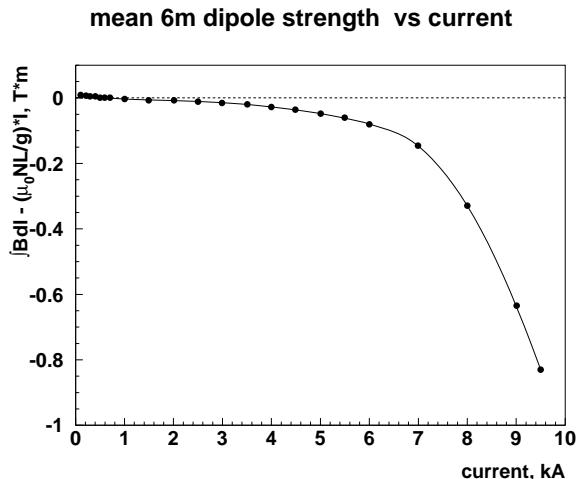


Figure 1. Deviation of average dipole strength from linear vs current

To present the magnet-to-magnet variation, we calculate the fractional deviation of individual magnets from the average. Figure 2 shows the strength at 1500 A for all magnets in the sample, relative to the average of all magnets except the first eight, whose measurements are significantly noisier than the later measurements. At this current the strength is dominated by the geometry, with only a small contribution from the permeability of the steel. Note that the strengths are tightly clustered, indicating good control of the geometry. All magnets fall within the expected range.

Figure 3 shows the strength at 9500 A (a little over full excitation) for all magnets in the sample relative to the average of all magnets except the first eight. Note that the local average of the strengths started to increase about half way into this group of magnets. Although no magnet falls outside the acceptable range, it is important to understand and control the process so that the variation does not increase further.

The nature of the increase can be better appreciated by looking at the relative strength as a function of current for a limited number of magnets, as shown in Figure 4. Here we see that the strength deviation depends on current, a strong indication that

we are seeing a magnetic property of the steel, as opposed to a geometrical effect.

Analyzing the composition of the magnets, we determined that the strength deviation of the magnet was closely correlated with the mix of laminations in the magnet stamped from different processing runs of steel. A detailed examination of the magnetic data on the sample strips from steel coils shows statistically significant differences among the runs of steel. Two-dimensional modeling of the magnetic field using the different B-H curves reproduces the differing magnet excitation curves.

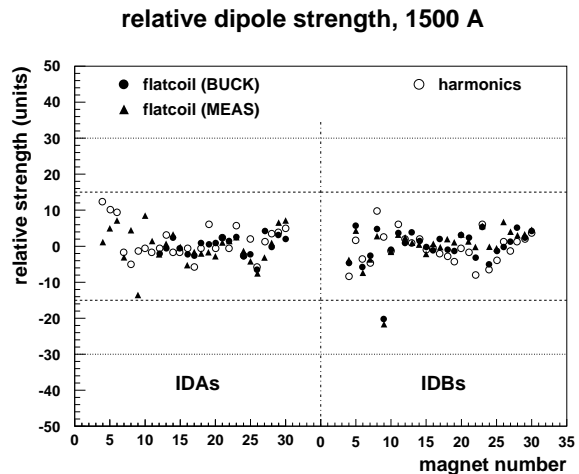


Figure 2. Relative strength of all dipoles at 1500 A

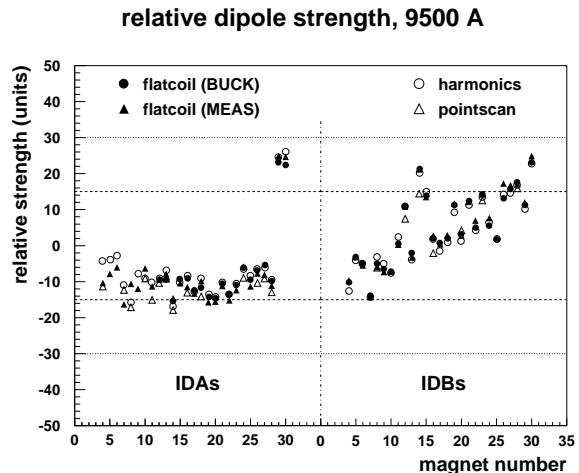


Figure 3. Relative strength of all dipoles at 9500 A

#### B. Shape

The complementary measurement techniques, flatcoil and harmonics, give consistent results. Figure 5 shows the average  $b_3$  as a function of current. This is consistent with calculations and with the performance of the prototype dipoles, upon which the chromaticity sextupole design was based.

The sextupole components at 9500 A are histogrammed in Figure 6. All magnets fall well within the expected range of values. The distribution of the decapole component at 9500 A is shown in Figure 7. All magnets are within the established limits.

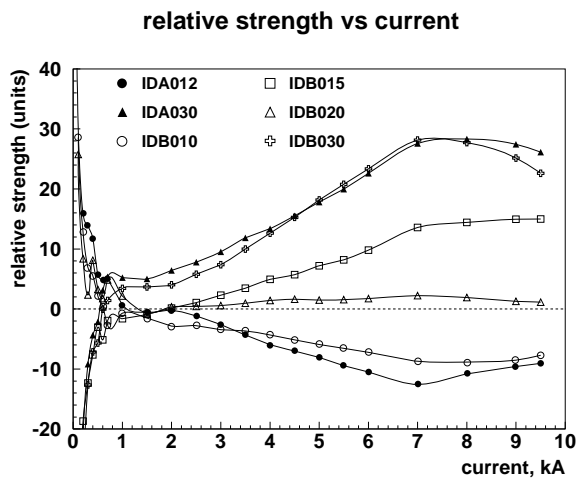


Figure 4. Relative strength of representative dipoles as a function of current

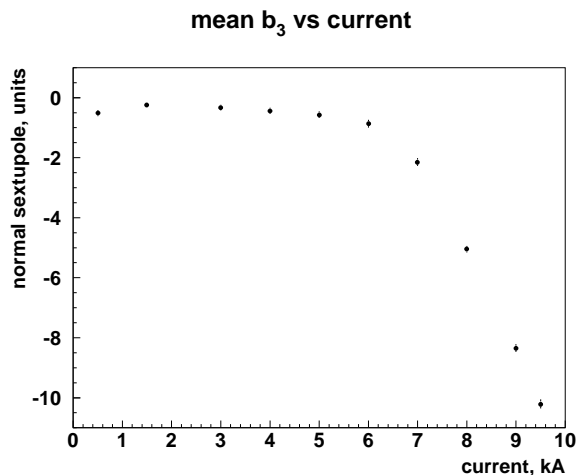


Figure 5. Average sextupole component vs current

#### IV. Conclusions

The Fermilab Main Injector project is well into production of dipoles for the ring. By the end of March 1995 54 6-m dipoles, out of 216 required for the ring, had been completed and measured. Magnet performance is within the acceptable range established through tracking studies.

#### References

- [1] D. Bogert. The Fermilab Injector Complex. In *Proceedings this conference*, 1995.
- [2] C.S. Mishra P.S. Martin D.J. Harding H.D. Glass and B.C.Brown. Fermilab Main Injector Magnet Acceptance Criteria. In *Proceedings this conference*, 1995.
- [3] C.S. Mishra. Simulation of the Fermilab Main Injector with Production Magnet Data. In *Proceedings this conference*, 1995.
- [4] C.M. Bhat et al. The Main Injector Chromaticity Correction Sextupole Magnets: Measurements and Operating Schemes. In *Proceedings this conference*, 1995.

$b_3$  distribution at 9500 A

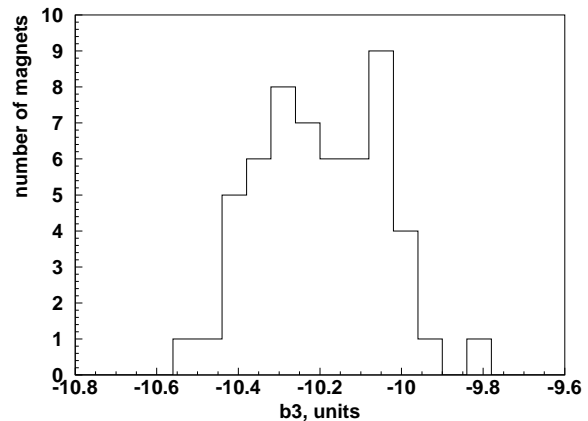


Figure 6. Distribution of sextupole strengths at 9500 A

$b_5$  distribution at 9500 A

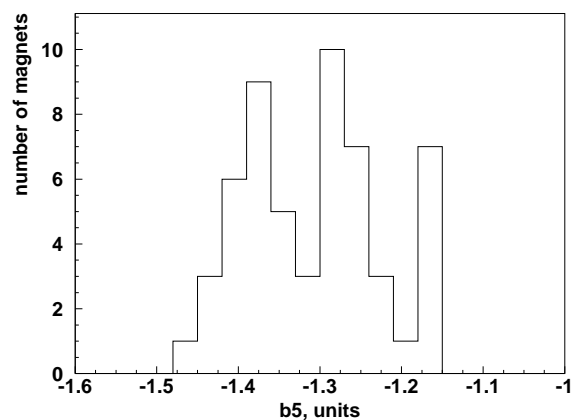


Figure 7. Distribution of decapole strengths at 9500 A

- [5] J.W. Sim et al. Software for a Database-Controlled Measurement System at the Fermilab Magnet Test Facility. In *Proceedings this conference*, 1995.